Pharm Res (2012) 29:1282–1294
DOI 10.1007/s11095-012-0678-8

RESEARCH PAPER

Targeted Endothelial Gene Delivery by Ultrasonic Destruction of Magnetic Microbubbles Carrying Lentiviral Vectors

Hanna Mannell • Joachim Pircher • Thomas Räthel • Katharina Schilberg • Katrin Zimmermann • Alexander Pfeifer • Olga Mykhaylyk • Bernhard Gleich • Ulrich Pohl • Florian Krötz

Received: 1 August 2011 / Accepted: 6 January 2012 / Published online: 25 January 2012

ABSTRACT

Purpose Site specific vascular gene delivery is a promising tool for treatment of cardiovascular diseases. By combining ultrasound mediated microbubble destruction with site specific magnetic targeting of lentiviruses, we aimed to develop a technique suitable for systemic application.

Methods The magnetic nanoparticle coupling to lipid microbubbles was confirmed by absorbance measurements. Association of fluorescent lentivirus to magnetic microbubbles (MMB) was determined by microscopy and flow cytometry. Functionality and efficiency of GFP-encoding lentiviral MMB transduction was evaluated by endothelial (HMEC) GFP expression and cytotoxicity was measured by MTT reduction.

Results Microbubbles with a mean diameter of 4.3 ± 0.04 μm were stable for 2 days, readily magnetizable and magnetically steerable *in vitro* and efficiently associated with lentivirus. Exposure of eGFP-encoding lentiviral MMB to human endothelial cells followed by application of an external static magnetic field (30 min) and ultrasonic destruction of the microbubbles did not markedly affect cellular viability. Finally, this combination led to a 30-fold increase in transduction efficiency compared to application of naked virus alone.

Conclusions By associating microbubbles with magnetic iron nanoparticles, these function as carriers for lentiviruses achieving tissue specific deposition at the site of interest.

KEY WORDS endothelial cells · gene delivery · lentiviral transduction · magnetic nanoparticles · microbubbles · ultrasound

ABBREVIATIONS

DC	duty cycle
LV	lentivirus
MF	magnetic field
MMB	magnetic microbubbles
MNP	magnetic nanoparticles
US	ultrasound

INTRODUCTION

In vascular research, therapeutic gene delivery by viruses constitutes an elegant way to specifically modulate signalling molecules and physiological responses. However, this technology needs to be improved regarding undesired side effects, transfection efficiency and targeted delivery. The vascular system in general would represent an ideal route for transporting drugs and genetic material to a specific site of therapeutical intervention *in vivo*. However, systemic

H. Mannell • U. Pohl
Walter-Brendel-Centre of Experimental Medicine
Schillerstrasse 44
80336 Munich, Germany

J. Pircher • T. Räthel • K. Schilberg • F. Krötz (✉)
Cardiology, Medical Policlinic, Ludwig-Maximilians-University
Ziemssenstrasse 1
80336 Munich, Germany
e-mail: floriankroetz@gmx.de

K. Zimmermann • A. Pfeifer
Institute of Pharmacology and Toxicology
Biomedical Center University of Bonn
Sigmund-Freud-Straße 25
53105 Bonn, Germany

O. Mykhaylyk
Institute of Experimental Oncology and Therapy Research
Technische Universität München
Ismaninger Str. 22
Munich 81675, Germany

B. Gleich
Central Institute of Medical Engineering (IMETUM)
Technische Universität München
Boltzmannstr. 11
85748 Garching, Germany

application of viruses results in their dilution in the blood volume. In addition they interact with blood cells, antibodies and blood factors, which prevents efficient delivery to the site of desire (1). Moreover, systemic vascular application results in non-specific distribution of viruses, which in turn give rise to undesired side effects. Lentiviral gene transfer has the ability to achieve long-term therapeutic effects and satisfying gene expression generating physiological responses (2). Furthermore, lentiviral transduction is suitable for gene delivery to cells of the vascular system, which seldom divide (3), as lentiviruses are independent of cell divisions to deliver their genetic material. Targeted delivery by ultrasound mediated gene transfer using microbubbles as carriers of viral vectors is a promising concept and might be used to achieve targeted delivery and release of lentiviral particles. Indeed, this system has been used in several studies to deliver genes of interest to specific sites of the vasculature (4–8). Combining ultrasonic microbubble technology with the principle of magnetic nanoparticle (MNP)-assisted gene delivery (9,10), however, could even further enhance the efficiency and the specificity of cell and tissue transduction. Magnetic microbubbles, targeted to the site of interest by application of an external magnetic field, could result in a drug carrier system that can be transported with the blood flow (11). Therefore, we sought to establish a method for site directed gene delivery to the endothelium, which may also be a suitable tool for gene transfer *in vivo*. This was achieved by associating lentiviral particles to magnetic (MNP) perfluorocarbon-filled lipid microbubbles and combining magnetic targeting of these complexes with ultrasound mediated microbubble rupture.

MATERIALS AND METHODS

Chemicals

1,2-Bis(diphenylphosphino)ethane (DPPE) and dipalmitoylphosphatidylcholine (DPPC) of pharmaceutical grade quality were purchased from Lipoid GmbH (Ludwigshafen, Germany). Green fluorescent magnetic nanoparticles (nano-screenMAG/G-UC/C) were a kind gift from Dr. C. Bergemann. All other chemicals were from Sigma-Aldrich (Taufkirchen, Germany).

Lentiviral Constructs

Production and preparation of the lentiviral particles rrl-CMV-eGFP as well as the non integrating fluorescent labeled lentiviral particles pCHIV.eGFP (12) were performed as previously described (13). Briefly, HEK293T producer cells at ca. 50% confluency were transfected by use of calcium phosphate with the lentiplasmid rrl-CMV-eGFP together with the structure and packaging plasmid encoding for VSV-G, rev and gag/pol. In case of pCHIV.eGFP transfection was performed with a plasmid mixture of pCHIV and pCHIVeGFP together with the plasmid encoding for VSV.G envelope. Medium was changed on the next day. Virus containing cell culture supernatant was each collected 48 h and 72 h after transfection and filtered using a 0.45 µm filter (SFCA, Nalgene, Thermo Fisher Scientific, Waltham, MA, USA) to remove cell debris. Viral particles were then concentrated by ultracentrifugation with a final centrifugation step on a 20% (w/v) sucrose cushion and resuspended in Hank's balanced salt solution (HBSS, Invitrogen, Darmstadt, Germany). The physical viral titer (in VP/ml) was calculated by measuring the activity of the reverse transcriptase as described by Trueck *et al.* (14) whereas the biological titer (in IP/ml) was determined by transduction of HEK293T cells and flow cytometry of transduced cells as described elsewhere (13).

Cell Lines and Cell Culture

Human dermal microvascular endothelial cells (HMEC) were cultured in DMEM supplemented with 10% fetal calf serum, 10% Endopan 3 (PAN Biotech, Aidenbach, Germany) and 1% penicillin-streptomycin in a humidified incubator at 37°C and 5% CO_2 as described previously (15).

MTT Assay

Cell viability was measured by incubation of cells in 0.5 mg/ml methyl thiazolyl tetrazolium, MTT, for 2 h at 37°C. Cells were then rinsed with phosphate buffered saline (PBS) and the formazan salt (reduced MTT) was solved in 100% 2-Propanol and the colour intensity measured at 550 nm and 620 nm with a SpectraFluor (Tecan, Crailsheim, Germany) as described previously (15). For data analysis the 620 nm values were subtracted from the 550 nm values and normalized to the values for non treated cells.

Synthesis of Magnetic Nanoparticles

Core-shell type iron oxide MNPs were synthesized by precipitation of Fe(II)/Fe(III) hydroxide from aqueous solution of the mixture of Fe(II) and Fe(III) salts, followed by transformation into magnetite in an oxygen-free atmosphere with spontaneous adsorption or condensation of shell components as described elsewhere (16–18). To modify the surface of the PEI-Mag2 and PEI-Mag3 magnetic nanoparticles the fluorinated surfactant ZONYL FSA (lithium 3-[2-(perfluoroalkyl)ethylthio]propionate) (FSA) was combined with 25-kDa branched polyethylenimine (PEI). The X-ray photoelectron data analysis resulted in 32% (w/w) PEI and 68% (w/w) FSA for PEI-Mag2 nanoparticles and 93.7% (w/w) PEI and 6.3% (w/w) FSA for PEI-Mag3 nanoparticles. Both particles have highly positive theta-potential (55.0±0.7 and

53.4±0.7 mV, respectively), saturation magnetization of the core of 62 and 34 emu/g iron and core diameter of 9 and 8 nm, respectively. To modify the surface of the magnetite nanoparticles PalD1-Mag4 and PalD2-Mag1 the fluorinated surfactant ZONYL FSE was combined with palmitoyl dextran PalD1 and PalD2, respectively. Palmitoyl dextran PalD1 and PalD2 with 11 and 32 palmitoyl groups per 100 dextran units were synthesized by means of esterification of Dextran-10 (Amersham Biosciences) with palmitoyl chloride (SigmaAldrich) as described elsewhere (19). MNP conjugated with fluorescent dye Atto-550-PEI-Mag2 (Atto-550, Sigma-Aldrich, Taufkirchen, Germany) were prepared by mixing 2 ml PEI-Mag2 nanoparticle suspension in water (2.5 mg Fe/ml) with 443 µl 0.1 M Na-Borate buffer, pH 8.5, and 57 µl solution of Atto-550 in DMSO (2 mg/ml). The resulting suspension was incubated overnight at room temperature and dialyzed using a Pierce cassette dialysis device with a cut-off at 3,500 MW. The resulting suspension contained 2.7 mg Fe/ml. For determination of the immobilized dye concentration after extensive dialysis against water, the adsorbtion spectra of the diluted suspensions of dye-particles conjugates (about 80 µg Fe/ml) were measured in the range 300–800 nm using BECKMAN DU-600 spectrophotometer. Optical density at 555 nm was measured with correction for the adsorption of the particles and immobilized dye concentration per unit iron weight was calculated with account for the Atto-550 extinction coefficient at 555 nm of 120,000 (L/mol cm) and iron concentration of the MNP suspension determined spectrophotometrically with o-phenantroline as described previously. The concentration of the dye conjugated with nanoparticles was 47 µM (or 1.4% based on iron weight or 15 dye molecules per insulated magnetic nanoparticle) as determined spectrophotometrically.

Preparation of Magnetic Microbubbles and Association of Lentiviral Particles

For 10 ml of microbubble solution, phospholipids (2 mg DPPE and 10 mg DPPC) were mixed in chloroform in a round bottom flask using rotation under heating at 60°C in a water bath. The organic solvent was then removed under vacuum using a Rotavapor-R (Büchi Labortechnik GmbH, Essen, Germany) and the remaining lipids were dissolved in 10% glycerol at 60°C in a water bath under rotation. If not otherwise stated, 250 µg magnetic iron oxide nanoparticles were mixed with the lipid solution in 1.5 ml glass vials with screw caps with silicon/PTFE membranes (Schubert & Weiss Omnilab GmbH, München, Germany). The mixture was then covered with perfluorocarbon gas and shaken for 20 s in a CapMix (3 M ESPE, Seefeld, Germany). For coating with lentiviral particles, viral particles were added to magnetic microbubbles and the mixture was coated with gas and left to incubate for 10 min before use. The formation of microbubbles was confirmed by microscopy and by applying pressure to the mixture forcing the microbubbles to rupture leaving a clear solution. The association of pCHIV.eGFP viral particles to magnetic microbubbles was controlled for by fluorescence microscopy (Axiovert 200M microscope Zeiss, Jena, Germany) and flow cytometry.

Measurement of Magnetizability and Size of Microbubbles

Microbubbles coated with magnetic particles were exposed to a magnetic field and the kinetics of the suspension clearance was measured at 480 nm with a modified Specord 210 (Analytik Jena, Jena, Germany). The microbubbles' size was assessed by microscopy as well as with a Casy Counter (Schärfe Systems, Roche Diagnostics, Mannheim, Germany).

In Vitro Transduction and Transduction Efficiency Experiments

For transduction of lentiviral particles associated to magnetic microbubbles a magnetic nanoparticle to lentiviral particle ratio of 300 fg Fe/viral particle to match a multiplicity of infection (MOI) of 5, if not stated otherwise, was used. Viral magnetic microbubbles (MMB) were applied to subconfluent HMEC in DMEM supplemented with 1% fetal calf serum. The cell plate was placed on top of a neodymium iron boron magnet and the cells sonicated (1 MHz ultrasound frequency with an exposure time of 0.5 min at an intensity of 2 W/cm^2 and 50% duty cycle) by applying the ultrasound probe directly into the medium using an ultrasonic device from Rich-mar (G. Heinemann, Schwaebisch Gmuend, Germany) followed by further incubation on the magnet for 30 min at 37°C under static conditions. The cells were then rinsed with PBS and cultured in 10% HMEC medium for another 72 h. For measurement of transduction efficiency transduced cells (HMEC) were washed with PBS followed by detachment from the culture dishes with Accutase. Cells were pelleted at 0.8 g for 2 min and pellets rinsed with PBS followed by fixation in 3% formalin without methanol for 10 min. Following rinsing with PBS the cells were suspended in PBS and the expression of eGFP was measured using a FACS Canto II (BD Biosciences, Heidelberg, Germany). eGFP expression was also confirmed by fluorescent microscopy. The fluorescence intensity was evaluated within regions of interest (entire image).

Statistical Analysis

All statistical analyses were performed using Sigma Plot version 10.0. For comparisons of two normally distributed

groups of data, the Student's *t*-test was used. For multiple comparisons of normal distributed data the one-way analysis of variance (one-way ANOVA) was used. All data are presented as means±SEM. Differences were considered significant at an error probability level of $p<0.05$.

RESULTS

Characteristics of Microbubbles

The microbubbles generated in this study were shown to have a mean diameter of 4.3±0.04 µm and upon association with different MNP the mean diameter was kept constant. Only in the case of coating with PEI-Mag2 the diameter was increased (4.6±0.02 µm, $p<0.05$, $n=3$, Table 1) compared to naked microbubbles. Interestingly, when coating with positively charged PEI-Mag2 and PEI-Mag3 the amount of microbubbles/ml was not significantly changed, although somewhat lower in comparison to naked microbubbles (Table 1, $n=3$). However, when coating with the negatively charged MNP PalD2-Mag1 or PalD1-Mag4 the amount of microbubbles/ml was significantly reduced compared to the amount of naked microbubbles/ml ($p<0.05$, $n=3$, Table 1). The microbubbles remained stable for up to 48 h under perfluorocarbon gas (Fig. 1a, $n=3$). For efficient rupture of magnetic microbubbles (MMB), different times of ultrasound exposure were tested while keeping the frequency, intensity and duty cycle constant (1 MHz, 2 W/cm^2, DC 50% respectively). As shown in Fig. 1b all exposure times tested efficiently destroyed the microbubbles, as assessed by microscopy ($n=3$). To evaluate the effect of ultrasound exposure on cell viability, human microvascular endothelial cells (HMEC) were exposed to ultrasound for the different times and the cytotoxicity measured directly after treatment by MTT reduction. As seen in Fig. 1c, an exposure time of 0.5, 1, 2 and 3 min did not have a significant impact on cell viability although a tendency towards a time dependent reduction in cell viability was observed ($n=12$, HMEC). 5 min of ultrasound treatment however, significantly affected cell viability ($p<0.05$, $n=12$, HMEC). Due to these results an ultrasound exposure of 0.5 min was chosen for the following experiments. Upon ultrasound application (1 MHz, intensity 2 W/cm^2, duty cycle of 50% and an exposure time of 0.5 min) 99.9%±2.8*10^{-4}% of the microbubbles were destroyed ($p<0.05$, $n=3$, Fig. 1a).

Table 1 Microbubble Size and Amounts

	Mean diameter (µM)	MB/ml
MB	4.3±0.04	48.2*10^6±5.5*10^6
MB + PEI-Mag2	4.6±0.02*	34.1*10^6±1.3*10^6
MB + PEI-Mag3	4.4±0.03	39.6*10^6±5.5*10^6
MB + Pald2-Mag1	4.3±0.02	17.0*10^6±0.4*10^6*
MB + Pald1-Mag4	4.3±0.00	22.2*10^6±1.3*10^6*

*$p<0.05$ vs MB; MB: Microbubbles

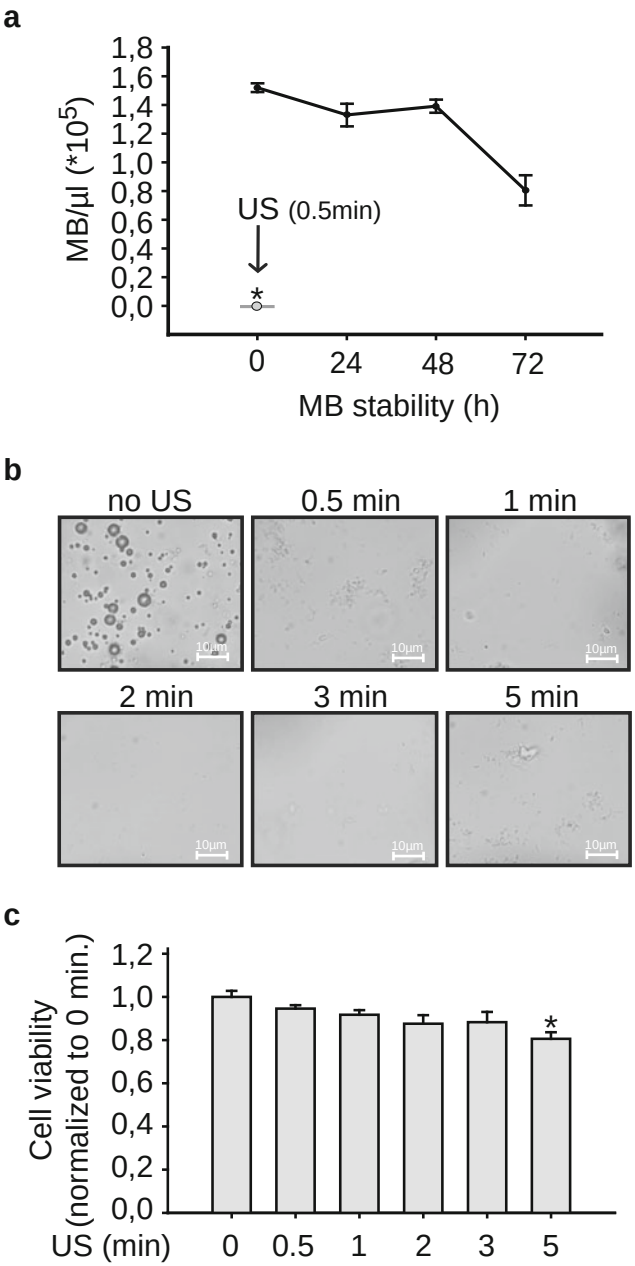

Fig. 1 Microbubble characteristics. (**a**) Microbubbles were shown to be stable up to 48 h ($n=3$) as measured by calculating the number of intact gas filled microbubbles at different time points. The majority of microbubbles were efficiently destroyed by ultrasound treatment with an exposure time of 0.5 min (*$p<0.05$, $n=3$). (**b**) Microscopic images of magnetic (PEI-Mag2) microbubbles before (far left) and after (right and second panel) different times of ultrasound treatment (1 MHz, 2 W/cm^2, DC 50%). (**c**) Cell viability upon different exposure times to ultrasound was measured by MTT reduction directly after treatment and the difference in viability was significant at the exposure time of 5 min (*$p<0.05$, 1 MHz, 2 W/cm^2, DC 50%, HMEC, $n=12$).

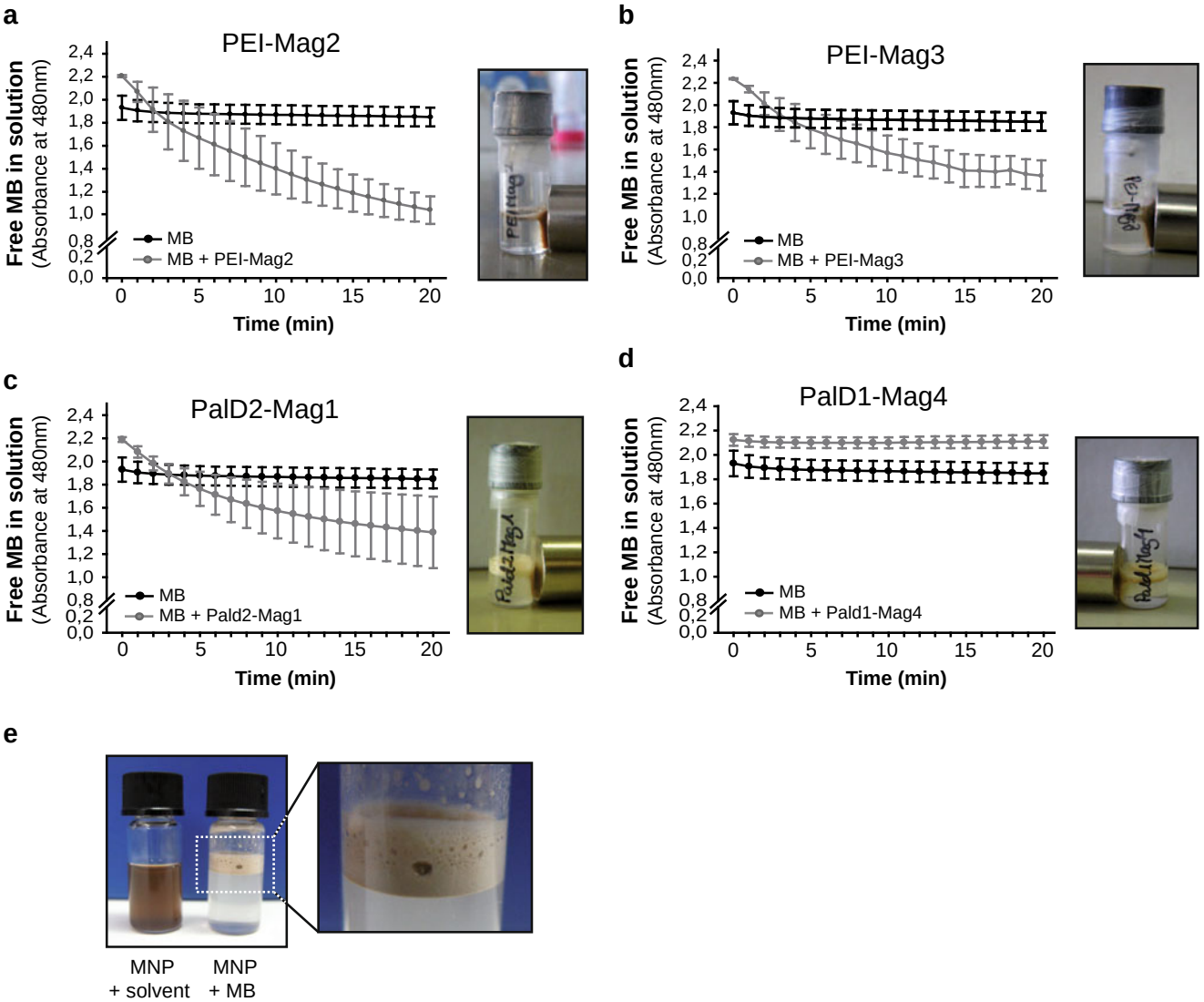

Fig. 2 Coating of microbubbles with magnetic nanoparticles. Microbubbles were made magnetic by coating with MNP (0.25 μg MNP/μl). The magnetizability was assessed by measurement of the clearance of the microbubble solution upon application of a magnetic field. Microbubbles were efficiently collected at the magnet when coated with (**a**) PEI-Mag2 (n=3) or (**b**) PEI-Mag3 (n=3). (**c**) Coating with PalD2-Mag1 (n=3) or (**d**) PalD1-Mag4 (n=3) was less efficient. Photos beside graphs show the collection of MMB upon application of an external magnetic field. (**d**) Added MNP associated with microbubbles as these could be observed to float to the surface together with the microbubbles (right vial) compared to solvent containing only MNP, where they remained homogenously solved (left vial, n=3). MB: Microbubbles, MNP: magnetic nanoparticles.

Synthesis of Magnetic Nanoparticle-Coated Microbubbles

Several MNP were tested for their ability to associate with microbubbles. To assess the binding of magnetic iron oxide nanoparticles to the lipid microbubbles the magnetizability of the microbubbles was measured by application of an external magnetic field generated by a neodymium iron-boron magnet. As seen in Fig. 2a–d (photos) the MMB were trapped at the site of the magnet and the rest of the solution remained clear. To quantify the magnetic responsiveness of the MMB, the turbidity of the solution was measured during the time of magnetic collection. Microbubbles coated with PEI-Mag2 and PEI-Mag3 were readily magnetizable compared to naked microbubbles, as shown by a faster collection time at the magnet, whereas coating with PalD2-Mag1 or PalD1-Mag4 was less efficient (n=3, Fig. 2a–d). To test the magnetic particle saturation of microbubbles to avoid rests of free MNP, they were left to stand for 1 h after coating with PEI-Mag2 to let the microbubbles float to the surface. As seen in Fig. 2e the MNP raised to the surface together with the microbubbles in contrast to MNP in the solvent not containing any microbubbles.

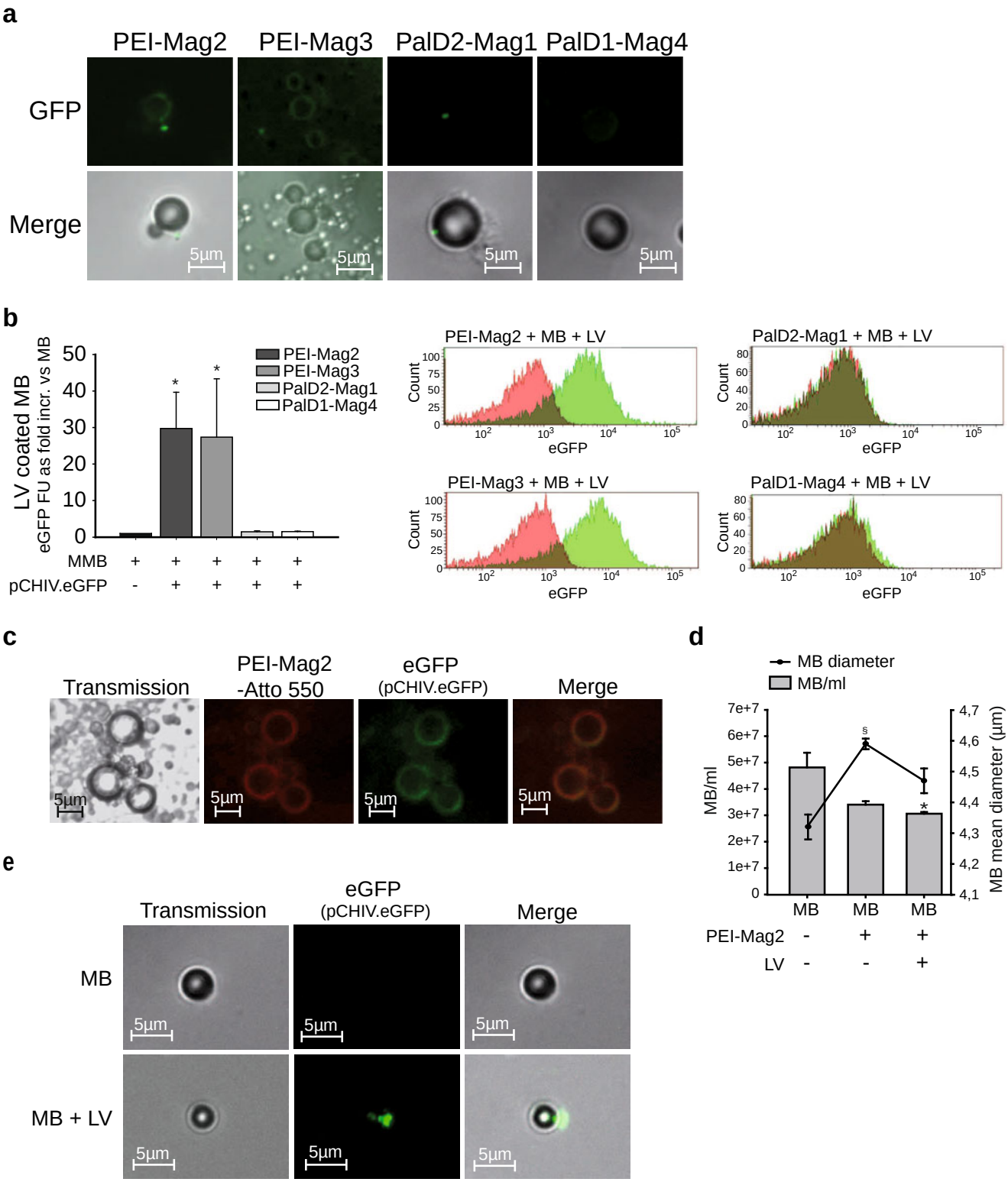

Association of Lentivirus to Magnetic Microbubbles

For lentiviral association to the microbubbles, a lentivirus carrying eGFP attached to the membrane bound matrix region of the structural HIV protein Gag (pCHIV.eGFP) (12) was used. Microbubbles coated with PEI-Mag2, PEI-Mag3, PalD2-Mag1 or PalD1-Mag4 were incubated with lentiviral particles for 10 min at room temperature and tested for binding of lentivirus by microscopy. As seen in Fig. 3a pCHIV.eGFP (green) attached efficiently to microbubbles

◀ **Fig. 3** Association of lentivirus to magnetic nanoparticles. (**a**) Magnetic microbubbles (MB, 0.25 μg MNP/μl) were incubated with a lentivirus (LV) containing a membrane GFP-fusion protein (pCHIV.eGFP) and the association was visualised by fluorescent microscopy. Microbubbles coated with the MNP PEI-Mag2 or PEI-Mag3 readily bound lentivirus, whereas coating with PalD2-Mag1 or PalD1-Mag4 did not associate with any detectable amounts of lentiviral particles (all $n=3$). (**b**) Flow cytometry analysis of these MMB revealed association of lentivirus when using PEI-Mag2 and PEI-Mag3 coated microbubbles (*$p<0.05$, $n=3$). PalD2-Mag1 or PalD1-Mag4 coated microbubbles did not associate with lentivirus ($n=3$). Histograms show the shift in GFP-fluorescence between MMB without pCHIV.eGFP (red) and with association of pCHIV.eGFP (green). (**c**) Association of lentivirus and MMB was visualised by fluorescence microscopy of microbubbles coated with fluorescently labelled PEI-Mag2 (PEI-Mag2-Atto-550, red) and fluorescent lentiviral particles (pCHIV.eGFP, green) ($n=3$). (**d**) The mean microbubble diameter was increased when coating with PEI-Mag-2 but not when adding lentiviral particles to the complex (§$p<0.05$, *vs.* naked MB mean diameter, black line, $n=3$), whereas the amount of microbubbles/ml was lower after lentiviral particle association (*$p<0.05$ *vs.* naked MB, grey bars, $n=3$). (**e**) Lentiviral particles (pCHIV.eGFP) associate directly with the microbubbles only to some extent as shown by the sparse green fluorescence surrounding the microbubbles. MB: microbubbles, LV: lentivirus.

coated with PEI-Mag2 or PEI-Mag3 but less efficiently to microbubbles coated with PalD2-Mag1 or PalD1-Mag4. The association of lentivirus was confirmed by flow cytometry showing significant binding of pCHIV.eGFP to microbubbles coated with PEI-Mag2 or PEI-Mag3 (Fig. 3b, $p<0.05$, $n=3$) in contrast to microbubbles coated with PalD2-Mag1 or PalD1-Mag4 ($n=3$). To study whether coupling of lentivirus affects the association of MNP to the microbubbles, fluorescently labeled MNP (Atto550-PEI-Mag2) were incubated with pCHIV.eGFP and the association of both magnetic particles and lentivirus was visualized by fluorescent microscopy. As seen in Fig. 3c both MNP as well as lentivirus associated with the microbubbles ($n=3$). The mean microbubble diameter or the amount of microbubbles/ml was not changed after lentiviral association in comparison to non viral MMB ($n=3$). However, compared to naked microbubbles, the amount of microbubbles/ml was significantly reduced (Fig. 3d, $p<0.05$, $n=3$). Furthermore, to elucidate whether the lentiviral particles associate with the MNP or the microbubbles, pCHIV.eGFP lentivirus was incubated with naked microbubbles and analyzed with fluorescence microscopy. Although a direct association of lentivirus with microbubbles was observed to some extent it was not as extensive as in combination with MNP (Fig. 3e).

Transduction Efficiency of Lentiviral Microbubbles Coated with Different Magnetic Nanoparticles

To investigate the functional capacity of this association, microbubbles coated with the four different MNP were incubated with a lentivirus carrying a CMV-driven eGFP expression cassette and applied to human microvascular endothelial cells (HMEC) followed by exposure to an external magnetic field for 30 min and ultrasound (Fig. 4a). These cells represent a feasible target of vascular gene delivery *in vivo*, since microvascular endothelial cells constitute the major part of the vascular network in tissues and are metabolically active. Transduction of HMEC with microbubbles coated with PEI-Mag2 or PEI-Mag3 resulted in a strong eGFP expression, whereas transduction with PalD2-Mag1 or PalD1-Mag4 coated microbubbles did not yield any higher eGFP expression than cells transduced with virus only (Fig. 4b and c, $n=4$). Due to these results and the data for the magnetizeability of the different nanoparticle coated microbubbles, the following experiments were performed using PEI-Mag2 nanoparticles. To confirm the association of lentivirus with MMB, we compared the transduction efficiency of endothelial cells (HMEC) through addition of lentiviral MMB with the addition of the supernatant left after magnetic collection of the microbubbles. As seen in Fig. 4c transduction of HMEC with the lentiviral MMB before magnetic separation, thus containing both magnetic microbubbles and lentiviral particles, resulted in expression of eGFP, whereas transduction using the supernatant after magnetic separation, not containing any MMB, did not yield any eGFP expression ($n=8$), demonstrating the association of lentivirus to MMB.

Magnetic Trapping and Ultrasound-Mediated Destruction of Microbubbles Enhances Lentiviral Transduction *In Vitro*

After establishing the optimal combination of lentivirus, MNP and microbubbles, we investigated the influence of the different parameters constituting this technique on endothelial lentiviral transduction. HMEC were transduced with lentivirus associated to magnetic (PEI-Mag2) microbubbles followed by exposure to a magnetic field and ultrasound application. The fluorescence intensity was measured 72 h following transduction by flow cytometry. Cells transduced with lentivirus without MMB did not express eGFP as compared to non transduced cells (Fig. 5a and b, $n=12$). Cells treated with lentiviral MMB without magnetic field exposure or with ultrasound application only showed a significantly higher eGFP expression ($p<0.05$, $n=12$, HMEC). However, treatment with lentivirus bound to MMB upon ultrasound in combination with magnetic field exposure for 30 min showed an even higher expression of eGFP compared to the other treatments ($53\pm0.6\%$ and $39\pm0.5\%$ enhancement respectively) or non transduced cells ($p<0.05$, $n=12$). These effects were also observed when performing fluorescent microscopy of cells undergoing the different treatments (Fig. 5c, $n=6$, HMEC). To control for these effects microbubbles coated with fluorescently labeled MNP were applied to endothelial cells using these settings.

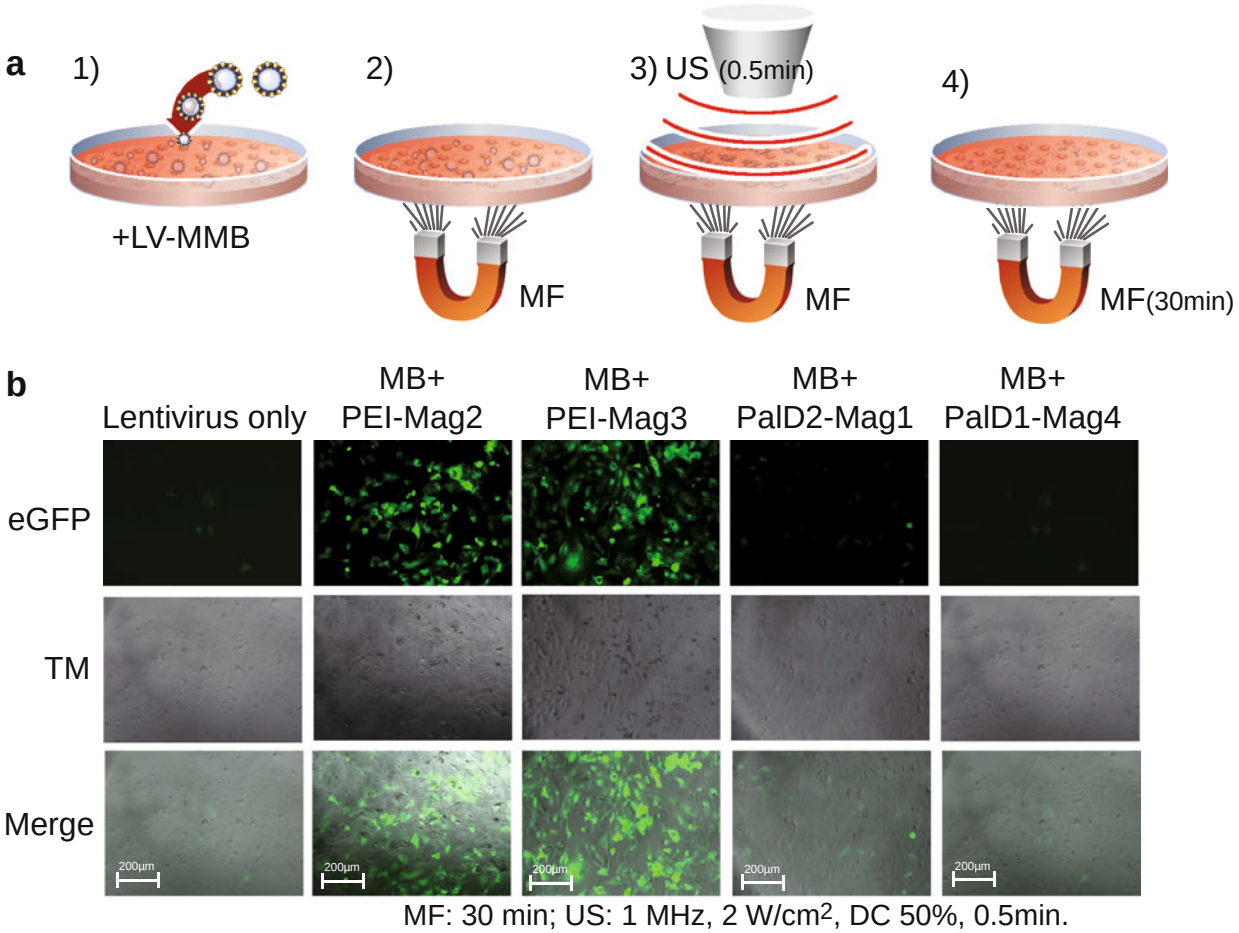
a
1)
+LV-MMB
2)
MF
3) US (0.5min)
MF
4)
MF(30min)
b
Lentivirus only
MB+ PEI-Mag2
MB+ PEI-Mag3
MB+ PalD2-Mag1
MB+ PalD1-Mag4
eGFP
TM
Merge
200μm
MF: 30 min; US: 1 MHz, 2 W/cm2, DC 50%, 0.5min.
c
eGFP expression (relative fluorescence intensity)
180
160
140
120
100
80
60
40
20
0
*
*
Lentivirus only
MB+PEI-Mag2
MB+PEI-Mag3
MB+PalD2-Mag1
MB+PalD1-Mag4
d
Before MF exposure
SN after MF exposure
eGFP
TM
Merge
200μm
PEI Mag2
PEI Mag3

◀ **Fig. 4** Functionality of lentiviral associated magnetic microbubbles. (**a**) Schematic drawing of magnetic microbubble mediated lentiviral transduction of endothelial cells. Addition of lentiviral MMB to the cell culture medium (1) is followed by application of a magnetic field, MF, (2) to allow for deposition of MMB on the cells. The MMB are destroyed by application of ultrasound, US, (1 MHz, 2 W/cm^2, DC 50%, 0.5 min) by immersing the probe into the medium (3). After US treatment the cells are left on the magnet for another 30 min (4). (**b**) Functionality of different MMB associated with a lentivirus containing a vector for eGFP-expression (rrl-CMV-eGFP, MOI 5) was measured by transduction of HMEC using the microbubble technique combined with ultrasound treatment (1 MHz, 2 W/cm^2, DC 50%, 0.5 min) and exposure to a magnetic field for 30 min (n=4). MB: Microbubbles, TM: Transmission. (**c**) Relative fluorescence intensity was measured of microscopic images shown in B as an index of eGFP expression (*$p<0.05$ *vs.* virus treatment only, n=4, HMEC). (**d**) Analysis of lentiviral association to microbubbles coated with PEI-Mag2. HMECs were treated with MMB carrying rrl-CMV-eGFP lentivirus (MOI 2) before (left panel) and with the supernatant (SN) after (right panel) magnetic collection of the microbubbles (n=8). MF: Magnetic field, SN: Supernatant, TM: Transmission.

Only the combined exposure to a magnetic field and ultrasound accomplished a major increase in deposition of magnetic microbubbles, as seen by fluorescent microscopy (Fig. 5d, n=4, HMEC). Upon application of these different settings to endothelial cells and measurement of the reduction of MTT as an index of cell viability, ultrasound alone or ultrasound together with magnetic microbubble application but without magnetic field exposure reduced cell viability with only 3.1±1.9% and 10.9±2.7% respectively, although not significantly, in comparison to non treated control cells (n=12, HMEC). Viral particles alone or in combination with ultrasound application showed no significant effect on cell viability in comparison to non treated cells (6.9±2.2% and 2.6±1.9% reduction respectively, n=12, HMEC). The application of MMB associated with lentivirus in combination with ultra sound and magnetic field exposure resulted in a slight, non significant, increase of cell viability of 6.2±2.9% (Fig. 5e, n=12, HMEC).

DISCUSSION

Targeted site-directed therapy would be of advantage in several pathological conditions and is favourable due to the reduction or even prevention of undesirable systemic side effects. Furthermore, by deploying therapeutic substances only at the site of interest, lower doses of the agent would be necessary, which is not only cost effective but further reduces side effects. However, several factors, such as the binding of therapeutical agents to plasma proteins and moderate physiological response, limit this approach. In this study we developed a method, which shows promising characteristics for local lentiviral gene delivery *in vivo*, by combining for the first time magnetic targeting with microbubble assisted lentiviral gene delivery. We successfully produced MMB by coating microbubbles with MNP and accomplished the association of lentiviruses to these complexes.

The microbubbles generated in this study show characteristics favourable for *in vivo* use, as the microbubbles have a diameter of below 5 µm, which is similar to the erythrocytes with mean diameters of 6–8 µm. Furthermore the phospholipid composition of the microbubbles makes them flexible, also in a similar way to the erythrocytes, thereby enabling their passage through the capillary system. In another study of ours, we were able to show that the majority of MMB were retained at the site of a magnetic field under flow, demonstrating high probability of being able to be steered to a specific site within the vasculature *in vivo* (20). This in turn is a prerequisite for systemic delivery without undesired trapping of the substances at other sites. Coupling of small oligonucleotides (21), plasmid DNA (22) and viruses (13) to MNP and their subsequent attraction towards an external magnetic field have previously been used as transfection or transduction technique of cells *in vitro*. This technique displays several advantages in comparison to standard transfection techniques, such as rapid deposition of the material to the cells (within 5 min of application), low cytotoxicity due to the reduced transfection time and high transfection efficiency as a result of the strong magnetic retention of the genetic material (21). In fact, this technique has been shown to even be highly efficient for gene or oligonucleotide delivery to primary endothelial cells, which have shown to be hard to transfect (22). These are all favourable characteristics for *in vivo* use. However, due to the blood flow velocity *in vivo*, a sufficient magnetic moment is needed to retain the MNP at the site of magnetic field exposure. As the magnetic moment is proportional to their size, larger particles may be needed, which may limit the passage through smaller vessels like the capillaries. To overcome this, our approach aimed to reach a sufficient magnetic moment by coating microbubbles with MNP instead. This was achieved by spreading the magnetic particles over a greater surface area and at the same time yielding a greater collection of MNP to one microbubble unit. We compared microbubbles with different MNP and analysed their ability to be steered towards and trapped at the site of a magnetic field. By studying these parameters we found that microbubbles were more readily coated with the positively charged MNP PEI-Mag2 or PEI-Mag3 than with the negatively charged PalD2-Mag1 or PalD1-Mag4. This can probably be explained by the fact that the phospholipids surrounding the gas core are negatively charged. An association of negatively charged MNP and negatively charged microbubbles may nevertheless be possible when using a positively charged linker, like Ca^{2+}, as described in the study of Soetanto *et al.* (23).

Microbubble mediated delivery of viral vectors, including retroviral particles, has been performed by other groups

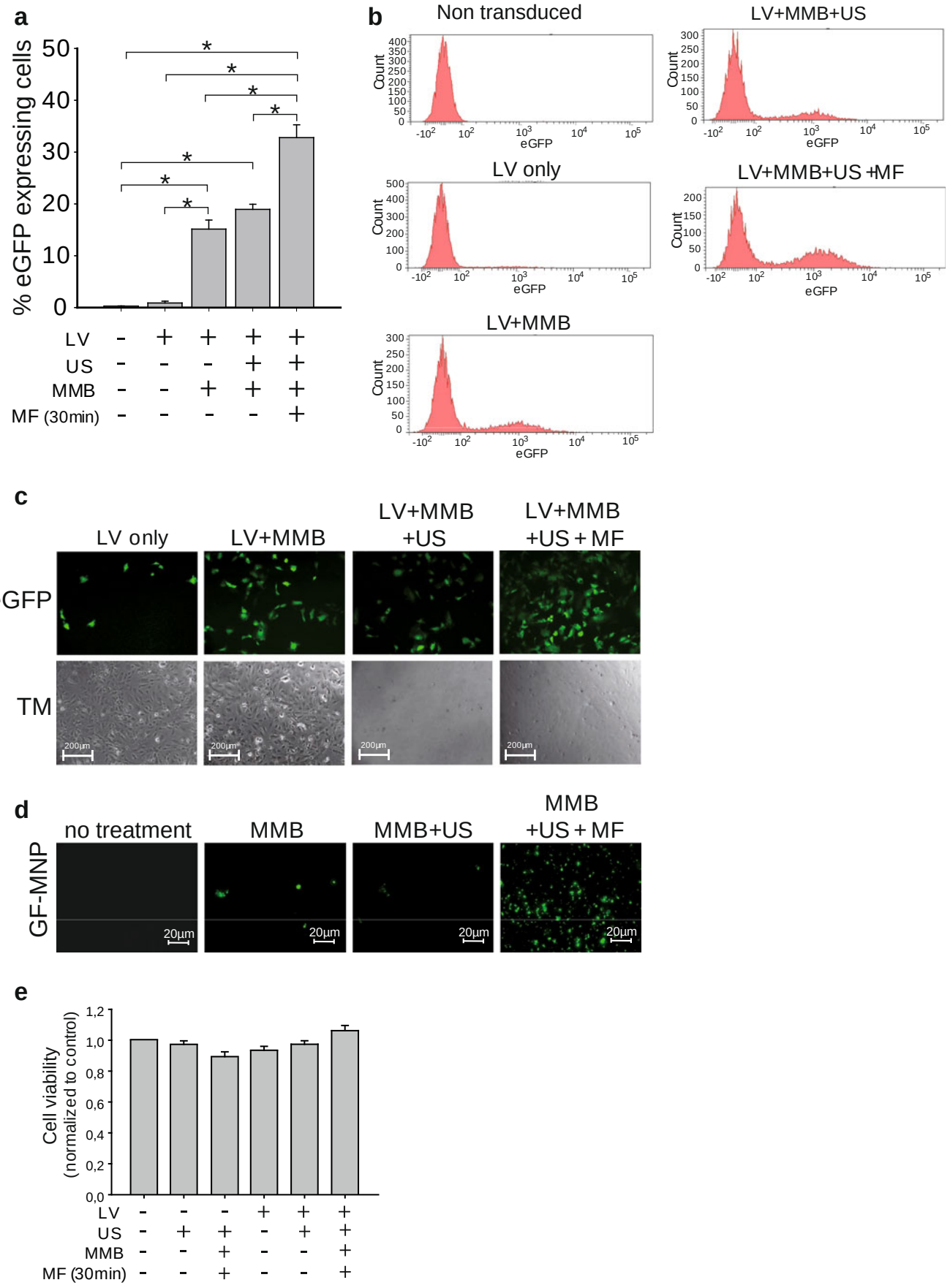
a
% eGFP expressing cells
LV
US
MMB
MF (30min)
b
Non transduced
LV+MMB+US
LV only
LV+MMB+US +MF
LV+MMB
Count
eGFP
c
LV only
LV+MMB
LV+MMB +US
LV+MMB +US + MF
eGFP
TM
200µm
d
no treatment
MMB
MMB+US
MMB +US + MF
GF-MNP
20µm
e
Cell viability (normalized to control)
LV
US
MMB
MF (30min)

◀ **Fig. 5** Magnetic trapping and ultrasound mediated destruction of microbubbles enhances lentiviral transduction *in vitro*. (**a**) Efficiency of different parameters constituting the MMB technique to transduce HMEC with rrl-CMV-eGFP (MOI 5) was measured by flow cytometry of eGFP expressing cells 72 h after transduction. While lentivirus (LV) alone (exposure time 30 min) did not result in any eGFP expression, exposure to lentiviral magnetic (PEI-Mag2) microbubbles or lentiviral MMB in combination with ultrasound (US) (1 Mhz, 2 W/cm^2, DC 50%, 0.5 min) enhanced the number of eGFP expressing endothelial cells. The highest eGFP expression was yielded when using the combination of lentiviral MMB, exposure of a magnetic field (MF) and US mediated MB destruction (*$p < 0.05$, $n=12$, HMEC). (**b**) Representative flow cytometry histograms showing the difference in amount of eGFP expressing cells using the different settings in **a**. (**c**) The transduction efficiency of the different combinations of MMB, MF and US exposure was confirmed by fluorescence microscopy ($n=6$, HMEC). TM: transmission. (**d**) Deposition of magnetic microbubbles on the cell surface was detected by fluorescence microscopy of microbubbles coated with fluorescent MNP (green) ($n=4$, HMEC). GF-MNP: Green fluorescent magnetic nanoparticles. (**e**) Cytotoxicity measurements of endothelial cells treated with different combinations of MMB, LV, US and MF assessed by MTT reduction 72 h after treatment (*$p < 0.05$, $n=12$, HMEC).

(24–26). By local ultrasound application relatively high specificity to the target site could be obtained. However, these microbubbles circulate freely and several runs of ultrasound application are therefore needed to efficiently destroy the majority of the microbubbles at a local site. By associating lentiviral particles to MMB, as performed in this study, these can be forced to deliver their genetic material to a specific site after magnetic trapping followed by ultrasound mediated destruction of the microbubbles. Our hypothesis was that the concentration of magnetic microbubbles at the site of interest during exposure to a magnetic field would be more rapid and further increased resulting in higher accumulation of the genetic material, which in turn would enhance gene transfer efficiency. Indeed, lentiviral particles readily and rapidly associated with the positively charged MMB probably through electrostatic interactions. In our microbubble complexes an association between the magnetic particles and the lentivirus takes place rather than a direct association of lentivirus to microbubbles, as this was shown to be rather poor. This indicates that the lentiviral particles are surrounding the microbubble rather than being contained within the microbubble core. This is in concordance with the study of Trueck *et al.* (14) demonstrating efficient binding of lentiviral particles to these MNP. However, even if lentiviral microbubbles coated with negatively charged MNP were shown to inefficiently deliver the genetic material, these MNP may bind lentiviral particles *per se*, as also described by Trueck *et al.* (14), by for instance hydrophobic interactions between the hydrophobic palmitoyl groups of the PalD-MNP and hydrophobic residues present on HIV-derived lentiviral particles or in the presence of two-valent cations. Alas, the combination of lipid microbubbles, MNP and lentiviral particles is likely somewhat more complex. Even if poorly associated to microbubbles, the remaining free negatively charged MNP did not seem to bind lentivirus in our setting, as the transduction efficiency using these complexes were as low as with virus alone. Therefore the microbubbles or the solvent in which the microbubbles are present (10% glycerol) may interfere with the direct association of negatively charged MNP and lentiviral particles. Furthermore, this finding correlates well with the observation that the coating of microbubbles with negatively charged MNP was less efficient and that the amount of microbubbles/ml was significantly reduced in these samples. None the less, association of lentivirus to MMB did not change the characteristics any further and MMB carrying lentivirus efficiently and fast delivered their material to endothelial cells in culture upon magnetic field exposure and ultrasound application. This resulted in relatively high transduction rates considering the short incubation time (30 min). To a significant lesser extent addition of lentiviral MMB without magnetic deposition and bursting led to enhanced lentiviral mediated eGFP expression, as did the addition of lentiviral MMB combined with ultrasound exposure. These results coincide with the studies of Stride *et al.* and Vlaskou *et al.*, where a combination of both ultrasound and magnetic field exposure led to enhanced transfer of plasmid DNA using magnetic microbubbles compared to ultrasound (9) or magnetic field exposure alone (9,10). Surprisingly, in our experiments there was no difference in gene delivery efficiency between application of MMB and MMB in combination with ultrasound treatment. This may be explained by the relatively short incubation time (compared to the incubation time of 24 h by standard transfection procedures), as the material, whether set free by ultrasound exposure or not, does not have time to come into sufficient contact with the cells. Furthermore, our ultrasound settings may not increase cell permeability to a high extent, although sufficient for rupture of the MMB. In addition, microbubbles coated with fluorescently labelled MNP only showed high deposition of magnetic microbubbles when using an external magnetic field, suggesting that the increase in transduction efficiency is mainly due to a more rapid and enhanced interaction between viral microbubbles and cells. Taken together, this demonstrates that by combining ultrasound mediated destruction of lentiviral magnetic microbubbles with magnetic trapping the time of transduction can be reduced and the efficiency significantly enhanced without the cost of higher cytotoxicity; a feature also advantageous for an *in vivo* application. In contrast to the study of Su *et al.* (27), where ultrasonic destruction of microbubbles resulted in a reduction of endothelial cell viability of 30%, we only observed a 11% decrease in cell viability. This may be due to lower cell permeability upon ultrasound exposure using our settings. In other previous studies ultrasonic microbubble transfection, using settings similar to this study, did not result in a high reduction of cell viability

(approximately 10%) (28,29). More importantly, the application of MMB in combination with magnetic trapping and ultrasonic destruction of these did not further decrease cell viability. In fact, none of the treatment combinations decreased cell viability any further than application of virus alone, suggesting there are no additional effects of the combined treatments.

Although this technique shows promising characteristics for *in vivo* use, it still remains to be investigated how efficient the technique will be for gene transfer *in vivo*. The possibility of local magnetic targeting of substances to tissues is dependent on the strength of the applied magnetic field. Since this decreases with increasing distance to the magnetic tip, magnetic targeting of deeper situated tissues or of structures situated deeper within an organ remains challenging. One approach to overcome this problem is addressed by previous studies (30,31) and ourselves (20), where nickel coated vascular stents were magnetizied by an external magnetic field thus influencing the original magnetic field and causing strong field gradients deeper into tissues. This approach in combination with magnetic microbubble mediated lentiviral gene delivery may be promising for targeting non superficial vessels and continuous to be the focus of our future work.

CONCLUSION

In this study we for the first time show that coating lipid microbubbles with MNP followed by association of lentiviruses to these complexes is possible and that this technique accomplishes high transduction rates of endothelial cells very fast at low cytotoxicity. We therefore think this novel technique may prove efficient as a tool for site specific lentiviral mediated delivery of genetic material to the vasculature *in vivo* after systemical application, by possibly reducing not only undesired gene expression at distant sites but also the amount of lentiviral particles needed for a physiological response.

ACKNOWLEDGMENTS & DISCLOSURES

This work was funded by the German Research Foundation (Deutsche Forschungsgemeinschaft, DFG) within the DFG Research Unit FOR917.

We thank Professor Kräusslich at the Department of Virology, University Clinic Heidelberg for kindly providing the pCHIV.eGFP lentiviral vector.

REFERENCES

1. Barry MA, Hofherr SE, Chen CY, Senac JS, Hillestad ML, Shashkova EV. Systemic delivery of therapeutic viruses. Curr Opin Mol Ther. 2009;11:411–20.
2. Pfeiferand A, Hofmann A. Lentiviral transgenesis. Methods Mol Biol. 2009;530:391–405.
3. Cines DB, Pollak ES, Buck CA, Loscalzo J, Zimmerman GA, McEver RP, Pober JS, Wick TM, Konkle BA, Schwartz BS, Barnathan ES, McCrae KR, Hug BA, Schmidt AM, Stern DM. Endothelial cells in physiology and in the pathophysiology of vascular disorders. Blood. 1998;91:3527–61.
4. Phillips L, Klibanov A, Wamhoff B, Hossack J. Targeted gene transfection from microbubbles into vascular smooth muscle cells using focused, ultrasound-mediated delivery. Ultrasound Med Biol. 2010;36:1470–80.
5. Zhou J, Wang Y, Xiong Y, Wang H, Feng Y, Chen J. Delivery of TFPI-2 using ultrasound with a microbubble agent (SonoVue) inhibits intimal hyperplasia after balloon injury in a rabbit carotid artery model. Ultrasound Med Biol. 2010;36:1876–83.
6. Tinkov S, Coester C, Serba S, Geis N, Katus H, Winter G, Bekeredjian R. New doxorubicin-loaded phospholipid microbubbles for targeted tumor therapy: *in-vivo* characterization. J Control Release. 2010;148:368–72.
7. Kondo I, Ohmori K, Oshita A, Takeuchi H, Fuke S, Shinomiya K, Noma T, Namba T, Kohno M. Treatment of acute myocardial infarction by hepatocyte growth factor gene transfer: the first demonstration of myocardial transfer of a "functional" gene using ultrasonic microbubble destruction. J Am Coll Cardiol. 2004;44:644–53.
8. Bekeredjian R, Chen S, Frenkel PA, Grayburn PA, Shohet RV. Ultrasound-targeted microbubble destruction can repeatedly direct highly specific plasmid expression to the heart. Circulation. 2003;108:1022–6.
9. Stride E, Porter C, Prieto AG, Pankhurst Q. Enhancement of microbubble mediated gene delivery by simultaneous exposure to ultrasonic and magnetic fields. Ultrasound Med Biol. 2009;35:861–8.
10. Vlaskou D, Pradhan P, Bergemann C, Klibanov AL, Hensel K, Schmitz G, Plank C, Mykhaylyk O. Magnetic microbubbles: magnetically targeted and ultrasound-triggered vectors for gene delivery *in vitro*. AIP Conf Proc. 2010;1311:485–94.
11. Liu Y, Miyoshi H, Nakamura M. Encapsulated ultrasound microbubbles: therapeutic application in drug/gene delivery. J Control Release. 2006;114:89–99.
12. Lampe M, Briggs J, Endress T, Glass B, Riegelsberger S, Krausslich H, Lamb D, Brauchle C, Muller B. Double-labelled HIV-1 particles for study of virus-cell interaction. Virology. 2007;360:92–104.
13. Hofmann A, Wenzel D, Becher UM, Freitag DF, Klein AM, Eberbeck D, Schulte M, Zimmermann K, Bergemann C, Gleich B, Roell W, Weyh T, Trahms L, Nickenig G, Fleischmann BK, Pfeifer A. Combined targeting of lentiviral vectors and positioning of transduced cells by magnetic nanoparticles. Proc Natl Acad Sci USA. 2009;106:44–9.
14. Trueck C, Zimmermann K, Mykhaylyk O, Anton M, Vosen S, Wenzel D, Fleischmann B, Pfeifer A. Optimization of magnetic nanoparticles assisted lentiviral gene transfer. Pharmaceut Res. In revision; 2011.
15. Mannell H, Hellwig N, Gloe T, Plank C, Sohn HY, Groesser L, Walzog B, Pohl U, Krotz F. Inhibition of the tyrosine phosphatase SHP-2 suppresses angiogenesis *in vitro* and *in vivo*. J Vasc Res. 2008;45:153–63.
16. Mykhaylyk O, Antequera Y, Vlaskou D, Plank C. Generation of magnetic nonviral gene transfer agents and magnetofection *in vitro*. Nat Protoc. 2007;2:2391–411.
17. Vlaskou D, Mykhaylyk O, Tresilwised N, Pithayanukul P, Möller W, Plank C. Magnetic nanoparticle formulations for DNA and siRNA delivery. J Magn Magn Mater. 2007;311:275–81.
18. Mykhaylyk O, Sanchez-Antequera Y, Vlaskou D, Hammerschmid E, Anton M, Zelphati O, Plank C. Liposomal magnetofection. Meth Mol Biol. 2010;605:487–525.
19. Mykhaylyk O, Zelphati O, Hammerschmid E, Anton M, Rosenecker J, Plank C. Recent advances in magnetofection and its potential to deliver siRNAs *in vitro*. Methods Mol Biol. 2009;487:111–46.
20. Räthel T, Mannell H, Gleich B, Pohl U, Krötz F. Magnetic stents retain nanoparticle-bound antirestenotic drugs transported by lipid microbubbles Pharmaceutical Research. Accepted, 2011.

21. Krotz F, de Wit C, Sohn HY, Zahler S, Gloe T, Pohl U, Plank C. Magnetofection–a highly efficient tool for antisense oligonucleotide delivery *in vitro* and *in vivo*. Mol Ther. 2003;7:700–10.
22. Krotz F, Sohn HY, Gloe T, Plank C, Pohl U. Magnetofection potentiates gene delivery to cultured endothelial cells. J Vasc Res. 2003;40:425–34.
23. Soetanto K. Development of magnetic microbubbles for Drug Delivery System (DDS). Jpn J Appl Phys. 2000;39:3230–2.
24. Shohet RV, Chen S, Zhou Y-T, Wang Z, Meidell RS, Unger RH, Grayburn PA. Echocardiographic destruction of albumin microbubbles directs gene delivery to the myocardium. Circulation. 2000;101:2554–6.
25. Beeri R, Guerrero JL, Supple G, Sullivan S, Levine RA, Hajjar RJ. New efficient catheter-based system for myocardial gene delivery. Circulation. 2002;106:1756–9.
26. Taylor S, Rahim A, Bush N, Bamber J, Porter C. Targeted retroviral gene delivery using ultrasound. J Gene Med. 2007;9:77–87.
27. Su C, Chang C, Wang H, Wu Y, Bettinger T, Tsai C, Yeh H. Ultrasonic microbubble-mediated gene delivery causes phenotypic changes of human aortic endothelial cells. Ultrasound Med Biol. 2010;36:449–58.
28. Wang Y, Xu H, Lu M, Tang Q. Expression of thymidine kinase mediated by a novel non-viral delivery system under the control of vascular endothelial growth factor receptor 2 promoter selectively kills human umbilical vein endothelial cells. World J Gastroenterol. 2008;14:224–30.
29. Meijering B, Henning R, Van Gilst W, Gavrilovic I, Van Wamel A, Deelman L. Optimization of ultrasound and microbubbles targeted gene delivery to cultured primary endothelial cells. J Drug Target. 2007;15:664–71.
30. Pislaru SV, Harbuzariu A, Gulati R, Witt T, Sandhu NP, Simari RD, Sandhu GS. Magnetically targeted endothelial cell localization in stented vessels. J Am Coll Cardiol. 2006;48:1839–45.
31. Chorny M, Fishbein I, Yellen BB, Alferiev IS, Bakay M, Ganta S, Adamo R, Amiji M, Friedman G, Levy RJ. Targeting stents with local delivery of paclitaxel-loaded magnetic nanoparticles using uniform fields. Proc Natl Acad Sci USA. 2010;107:8346–51.